Magnetic Resonance Imaging, Vol. 5, pp. 101–108, 1987
Printed in the USA.

0730-725X/87 $3.00 + .00

● *Original Contribution*

APPLICATION OF AN EQUIVALENT CIRCUIT TO SIGNAL-TO-NOISE CALCULATIONS IN MRI

JOHN G. VAN HETEREN, R. MARK HENKELMAN AND MICHAEL J. BRONSKILL

Department of Medical Biophysics, University of Toronto, and Ontario Cancer Institute, 500 Sherbourne St., Toronto, Ontario, Canada M4X 1K9

Transfer functions determined from the component values of an equivalent circuit are used to calculate the relative signal-to-noise ratio of rf coils for magnetic resonance imaging. Experimental verification of the method is obtained by directly measuring signals from three solenoidal coils and by measuring the signal-to-noise ratio of these solenoids. The transfer functions separate the total noise voltage into contributions from the coil resistance and contributions from magnetic and electric field interactions with the sample. The use of this technique in understanding and improving coil design is discussed.

Keywords: **rf coils; Signal-to-noise ratio; Electric fields; Magnetic fields.**

INTRODUCTION

The design of the rf receiver coil is a major factor in optimizing the signal-to-noise ratio (SNR) in magnetic resonance (MR) imaging. Both the characteristics of the coil alone and its electric and magnetic field interactions with the patient determine receiver performance. In our previous paper[1] we developed an equivalent circuit which accurately modelled these interactions over a wide range of frequencies and sample conductivities for a variety of coil geometries. In this paper, we use this model to calculate the noise voltages arising from the equivalent circuit resistances and, hence, the relative SNR of an rf coil tuned to operate in a magnetic resonance imager.

Early attempts[2–4] to calculate the SNR of the NMR experiment considered only the coil with no mention of the noise voltages created by electric and magnetic field interactions with a conducting sample. The effects on SNR of electric and magnetic field interactions with a sample were introduced by Hoult and Lauterbur[5] who calculated the magnetic field interaction with the sample for a simple geometry, and developed an expression relating the electric field interaction to the power deposition in a lossy dielectric. Other authors[6,7] have analyzed coil performance by measuring the change in the quality factor (Q) with the coil empty and loaded. They used the change in Q together with other qualitative arguments to estimate the fraction of the noise voltage due to magnetic field interactions. Hayes *et al.*[8] have stated that SNR performance of a coil is best indicated by the ratio of empty coil Q to loaded coil Q, provided that electric field effects are insignificant. They assumed that their "birdcage" coil had little electric field interaction with the patient because its resonant frequency (f_{res}) shifted, when loaded, in a manner similar to that of surface coils known to have small dielectric losses. Hayes and Axel[9] used a similar approach to analyze the performance of surface coils for MR imaging. All these papers ignore electric field interactions or deal with them only on a qualitative basis.

Sergiadis[10] introduced an "electrostatic quality factor" using a cylindrical model of the coil–patient geometry. This factor, based on the measured detuning of the loaded coil, was then used to quantify the electric field losses of the system. Detuning, or shift in the resonant frequency when the coil is loaded with the patient, can be positive or negative and is, in general, a combination of both magnetic and electric field

RECEIVED 3/20/86; ACCEPTED 9/30/86.
Acknowledgments—Financial support for this work was received from the Medical Research Council of Canada, the National Cancer Institute of Canada, and the Ontario Cancer Treatment and Research Foundation. J. G. van Heteren is a recipient of a studentship from the Medical Research Council of Canada.

Address correspondence to Michael J. Bronskill, Physics Division, Ontario Cancer Institute, 500 Sherbourne St., Toronto, Ontario, Canada M4X 1K9.

interactions with the patient. In our equivalent circuit model[1] there are three energy-dissipating circuit elements which introduce noise. A general treatment of the total noise voltage requires consideration of these three components (magnetic, electric and coil noise voltages) whose importance depends both on the magnitude of the three circuit resistances and on the propagation of voltages within the entire circuit.

An exact determination of the magnitudes of the three noise voltages for a coil circuit and a calculation of its relative SNR can be performed using the equivalent circuit shown in Fig. 1. This circuit is similar to our previous equivalent circuit,[1] but now includes an impedance matching network consisting of series tuning capacitors (C_s) and stray cable capacitance (C_c). The coil inductance is L, its series resistance is R_s and C_p is the parallel tuning capacitance. The coil's electric field interaction with the sample is modelled by C_1, C_2 and R_e. Magnetic field interactions with the sample are modelled by a dissipative inductive loop (Fig. 1 of Ref. 1) which is represented in Fig. 1 as an impedance, Z_{mag}, in series with L [using Eq. (2) of Ref. 1].

Although the SNR can be calculated across points A and B, it is worthwhile in this case to include the matching network and calculate the SNR across points G and H. This approach serves to "normalize" all noise voltages to the matched impedance (usually 50 Ω) and enables direct comparison to imaging experiments. An additional practical advantage of using points G and H is that the matching network of existing coils often cannot be removed easily to permit access to points A and B.

In the following section, the transfer functions required for calculating the signal and noise voltages at points G and H of Fig. 1 are presented. These transfer functions are then used to calculate the relative SNR. In the experimental section, the magnitude of the most important transfer function is measured and compared to the calculated value. A subsequent experiment compares the SNR measured in an MR imager for several coils to that calculated by this method.

THEORY

Transfer Functions

Transfer functions are a convenient means of relating the signal and noise voltages developed in the various equivalent circuit components to voltages across points G and H. The transfer function $F_1(\omega)$ relates the signal emf at the coil to the signal voltage at G and H. Since R_s and the real part of Z_{mag}, $\mathrm{Re}(Z_{\mathrm{mag}})$, are in series with L, $F_1(\omega)$ also is used to calculate the magnetic and coil noise voltages between points G and H. A different transfer function, $F_2(\omega)$, is required to determine the electric field interaction noise voltage across G and H because R_e is not in series with L.

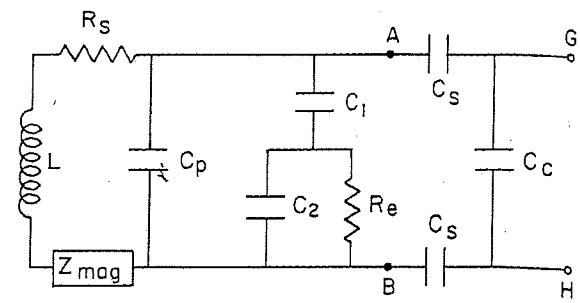

Fig. 1. Equivalent circuit which models a tuned MR imaging coil. This circuit includes an impedance matching network where C_c is the cable capacitance and C_s are series tuning capacitors. The coil is represented by L and R_s; C_p is the parallel tuning capacitance. Electric field interactions with the patient are modelled by C_1, C_2 and R_e. Magnetic interactions are modelled by Z_{mag}. The signal and noise voltages are calculated across points G and H.

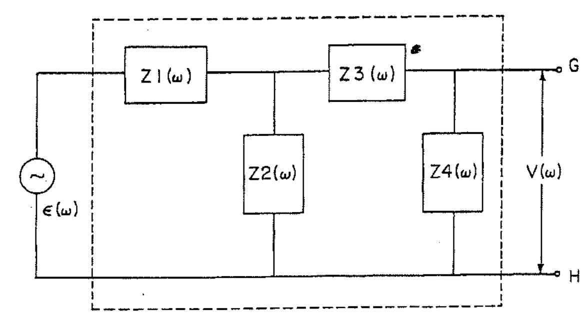

Fig. 2. The transfer function, $F_1(\omega)$ is calculated by grouping the impedances of Fig. 1 according to their series and parallel relationships for the voltage source and voltage measurement point. Note that both series matching capacitors, C_s, are grouped into $Z3(\omega)$.

The derivation of a transfer function is a straightforward procedure, and need not require complicated algebraic expressions. As an example, the derivation of $F_1(\omega)$ is shown below. The circuit components of Fig. 1 are first grouped into impedances according to their series and parallel relationships as shown in Fig. 2, where Z1–Z4 are defined by Eqs. (1)–(4).

$$Z1(\omega) = R_s + j\omega L + Z_{\mathrm{mag}}(\omega) \;, \tag{1}$$

$$Z2(\omega) = 1/\{j\omega C_p + 1/[1/(j\omega C_1) + 1/(1/R_e + j\omega C_2)]\} \;, \tag{2}$$

$$Z3(\omega) = 2/(j\omega C_s) \ , \tag{3}$$

$$Z4(\omega) = 1/(j\omega C_c) \ . \tag{4}$$

The transfer function, $F_1(\omega)$, relates the signal emf, $\epsilon(\omega)$, to the signal voltage across G and H, $V(\omega)$, and is calculated by applying Kirchoff's Laws to the circuit of Fig. 2, yielding

$$V(\omega) = \epsilon(\omega) F_1(\omega) \ ,$$

where

$$F_1(\omega) = \frac{Z4}{Z3 + Z4 + (Z2 + Z3 + Z4)(Z1/Z2)} \ . \tag{5}$$

A simple Fortran program can be used to evaluate $F_1(\omega)$. In this program, the known component values are inserted into Eqs. (1)–(4) to evaluate Z1–Z4. These impedances are then substituted into Eq. (5) to provide the value of F_1 for any frequency ω. $F_2(\omega)$ is evaluated in a similar manner.

Signal

The signal emf, $\epsilon(\omega)$, developed across the coil is transferred to points G and H by the transfer function $F_1(\omega)$. For MR imaging, the signal is spread over a sufficiently narrow frequency bandwidth (typically $\pm$ 10 kHz) that F_1 can be evaluated only at ω_0. In addition, the phase relationship between $\epsilon(\omega)$ and $V(\omega)$ is not important for this application. Thus the signal voltage transferred to points G and H is

$$V = \epsilon F_1 \tag{6}$$

where

$$F_1 = |F_1(\omega_0)| \ .$$

For simplicity, functions of frequency which are evaluated at ω_0 will be denoted similarly throughout this paper (e.g. F_2 means $|F_2(\omega_0)|$).

Noise

There are two ways of thinking about the total noise voltage and how it originates from the three resistive components [R_e, R_s and $\mathrm{Re}(Z_{\mathrm{mag}})$] of Fig. 1. In one method, the resistive components are considered individually, and their noise voltages transferred to points G and H are summed in quadrature. Alternatively, because the coil circuit is tuned to match a specific preamplifier impedance, the total noise voltage can be thought of as arising simply from the total real impedance across points G and H, $\mathrm{Re}(Z_{\mathrm{gh}})$. Thus two different coil systems tuned to 50 Ω will have the same total noise voltage and will differ only in the relative contribution of the noise voltages from R_e, $\mathrm{Re}(Z_{\mathrm{mag}})$ and R_s. These two approaches are mathematically equivalent and both are useful in understanding and optimizing coil performance.

The rms noise voltage developed across a resistance, R_s, is $(4\kappa T \Delta f R_s)^{1/2}$, where Δf is the frequency bandwidth, T is the conductor temperature and κ is Boltzman's constant.[11] This voltage is transferred to points G and H by F_1 to become a noise voltage equal to $F_1(4\kappa T \Delta f R_s)^{1/2}$. The rms noise voltages from the other resistive components are transferred to points G and H by their respective transfer functions. Since these voltages are uncorrelated, they must be summed in quadrature to obtain the total rms noise voltage, N_v, as shown in Eq. (7).

$$N_v = \{4\kappa T \Delta f (F_1^2(R_s + \mathrm{Re}(Z_{\mathrm{mag}})) + F_2^2 R_e)\}^{1/2} \ . \tag{7}$$

The alternative approach is to attribute N_v to the total real impedance $\mathrm{Re}(Z_{\mathrm{gh}})$ across points G and H. Thus

$$N_v = (4\kappa T \Delta f \ \mathrm{Re}(Z_{\mathrm{gh}}))^{1/2} \ . \tag{8}$$

Equations (7) and (8) are mathematically equivalent and yield the identical calculated value of N_v. The advantage of using Eq. (8) is that the noise can be interpreted as simply coming from the coil circuit impedance, regardless of the actual R_s, R_e and $\mathrm{Re}(Z_{\mathrm{mag}})$ values. Even for different receiver coils, the noise voltage at the preamplifier will be the same provided that all coils have the same $\mathrm{Re}(Z_{\mathrm{gh}})$. On the other hand, Eq. (7) is more useful in comparing the contributions to N_v from R_e, $\mathrm{Re}(Z_{\mathrm{mag}})$ and R_s.

Signal-to-Noise Ratio

The SNR at points G and H is obtained by dividing the signal voltage by the noise voltage. Thus the SNR in an image is calculated using Eq. (9), where N_v is determined from either Eqs. (7) or (8):

$$\mathrm{SNR} = \frac{F_1 \epsilon}{N_v} \ . \tag{9}$$

The signal emf in Eq. (9) depends on sample and magnetic field characteristics according to Eq. (10) developed by Hoult.[4]

$$\epsilon = \omega_0 B_1 M_0 V_s \cos \omega_0 t \ , \tag{10}$$

where ω_0 is the magnetic resonance frequency, M_0 is the sample magnetization, V_s is the sample volume and B_1 is the rf magnetic field strength in the transverse (xy) plane per unit current. Two factors (M_0, V_s) are constant for a given sample and ω_0 is constant at a particular operating frequency. Thus relative SNR can be calculated for a particular coil and sample as

$$\text{relative SNR} \propto F_1 B_1 / N_v \ . \tag{11}$$

In the next section this expression is verified experimentally, first by measuring the transfer function F_1, and then by measuring relative SNR in MR images for several coils. Under certain conditions Eq. (9) can be manipulated to agree with SNR expressions developed by other authors.[2,4] This relationship is investigated in the Appendix.

EXPERIMENTAL VERIFICATION

To test the accuracy of these equations, two experiments were performed using the three solenoid coils characterized earlier.[1] The first experiment verified the calculated magnitude of the transfer function F_1 by measuring the signal induced when these coils were placed in a uniform oscillating magnetic field. The second experiment compared the SNR measured from MR images to that calculated from Eq. (11).

The three solenoid coils were of the same length (2.5 cm) and diameter (2.5 cm), but differed in the number of turns and wire diameter giving variation in B_1 and R_s. Coil A had 7 turns of 2.8 mm diameter wire, coil B had 15 turns of 1.2 mm wire and coil C had 36 turns of 0.46 mm wire. The coils were tuned with series and parallel capacitors to resonate at 6.245 MHz, 57 Ω, with an 0.45 S/m NaCl solution sample (approximately physiological conductivity) inserted into the coil. A diode decoupler circuit[12] was added and the values of all the equivalent circuit components were determined by our conductivity variation technique.[1] The fitted parallel capacitance included the small capacitance of the diodes. The addition of C_s and C_p did not change the parameter values listed in Table 2a of Ref. 1.

Measurement of the Transfer Function

A signal emf ϵ was generated in the three solenoids by placing them in a uniform excitation magnetic field, B_e. This magnetic field was created by applying a voltage V_l at frequency ω_0 to a single turn, large diameter loop of impedance $|Z_l|$. The diameter of the loop, d_l, was chosen large enough to provide a uniform magnetic field at its center while minimizing interaction with the solenoid. At the center of this loop, $B_e = \mu_0 I/d_l$, where μ_0 is the permeability of free space, and $I = V_l/|Z_l|$ is the loop current. Thus the excitation magnetic field is given by

$$B_e = \mu_0 V_l / d_l |Z_l| \ . \tag{12}$$

The emf developed across an N-turn solenoid of area A_c placed at the center of the loop is $\epsilon = N \cdot A_c (dB_e/dt)$. Hence

$$\epsilon(\omega_0) = \frac{\mu_0 \omega_0 N A_c V_l}{d_l |Z_l|} \ . \tag{13}$$

This signal can be measured, after amplification by a factor A_v, as a voltage, V_{sig}. The amplifier loads the coil with an impedance Z_p placed across the capacitor C_c of Fig. 1. The calculated transfer function [F_1, Eq. (5)] is easily modified to include the effects of Z_p by placing the Z_p impedance in parallel with C_c in Eq. (4). The measured transfer function, $F_{1\text{meas}}$, can be evaluated from Eq. (14).

$$F_{1\text{meas}} = \frac{V_{sig}}{\epsilon} = \frac{V_{sig} d_l |Z_l|}{V_l \mu_0 \omega_0 N A_c A_v} \ . \tag{14}$$

Transfer Function Measurements

Experiments were performed using a 45-cm-diam loop ($|Z_l| = 63$ Ω) driven by a frequency synthesizer at 6.245 MHz at voltages V_l between 5 and 140 mV_{p-p}. The presence of this loop did not measurable alter the impedance of any of the solenoids. The area, A_c, of each solenoid was calculated from the coil former radius (1.27 cm) plus the radius of the wire (given in Table 1 of Ref. 1). The signal from each solenoid (with 0.45 S/m sample) was amplified by a broadband amplifier ($Z_p = 32$ Ω, $A_v = 13.9$) and measured on an accurately calibrated oscilloscope. The amplitude of the received signal was well below the diode threshold voltage; thus the decoupler circuit was not activated. The peak-to-peak signal amplitude measured on the oscilloscope, V_{sig}, was recorded for several values of V_l. $F_{1\text{meas}}$ was calculated from the slope of a graph of V_{sig}/V_l and the other constants shown in Eq. (14). The predicted and measured F_1 values are shown in Table 1 and agree within the error estimates for all three solenoids.

SNR Measurements

Experimental verification of Eq. (11) was performed by comparing the SNR measured in an MR imager to that predicted for the three coils. Each solenoid was positioned in a Technicare 0.15-T Teslacon imager with its magnetic field orthogonal to the transmit saddle coil's magnetic field. The solenoids were tuned to 57 Ω at 6.245 MHz such that a 53.5-Ω RG-55 quarter wavelength cable transformed the coil impedance to 50 Ω at the preamplifier input. A signal magnitude profile was obtained for a slice perpendicular

Table 1. Calculated and measured F_1

Coil	F_1* calculated from Eq. (5)	F_1† measured from Eq. (14)
A	7.41	7.76
B	3.26	3.54
C	1.05	1.00

*Based on $\mathrm{Re}(Z_p) = 32\ \Omega \pm 1\ \Omega$, the estimated error for F_1 calculated is 2%.
†Estimated error 5%.

to the solenoid axis, positioned in the middle of the solenoid. The amplitude of the 0.45 S/m NaCl sample's profile on a 4 average, TR = 2.0 sec, TE = 30 msec rf sequence was divided by the RMSD of the noise outside the profile to obtain the measured SNR as recommended by Edelstein *et al.*[13] The correction factor for magnitude reconstruction was negligible.[14] Each solenoid was positioned and measured 3 times and the average SNR and its uncertainty were determined.

The measured signal and noise data are shown in Table 2 along with the ratio of measured SNR to calculated SNR. Note that despite a five-fold variation in B_1, the SNR is very similar for these three coils. The measured noise values are almost equal, demonstrating that coils tuned to the same impedance have the same total noise voltage regardless of their R_s, R_e and $\mathrm{Re}(Z_{mag})$ values. The final column of Table 2 shows the ratio of measured to calculated SNR to be constant for the three coils, well within experimental error.

NOISE CONTRIBUTIONS

The transfer functions and circuit component values can be used [Eq. (7)] to calculate what fraction of the total noise voltage is due to the coil, electric field and magnetic field energy dissipating components. These noise voltage contributions are given in Table 3 for solenoids A–C in a 1-Hz bandwidth at the tuned resonance frequency of 6.245 MHz. As an interesting comparison, the noise voltages are also listed for the single turn half-saddle head coil (Coil E[1]). No uncertainties are listed in Table 3 because they are too difficult to calculate. The noise voltage uncertainties depend on the uncertainties in the values of the nonlinear system of components, some of which are coupled. The accuracy of the noise voltages determined with this technique is estimated to be a few percent.

For all coils in Table 3, the squares of the noise voltages sum to the same value, a consequence of having all coil circuits tuned to 57 Ω. At this frequency,

Table 2. Calculated and measured SNR

Coil	B_1 in mT/amp (±1%)	Calculated relative SNR $(F_1 \cdot B_1)$ (±3%)	Measured signal	Measured noise	Measured SNR (±5%)	Ratio: measured/calculated SNR (±8%)
A	0.234	17.3	214	0.189	1130	65.3
B	0.516	16.8	197	0.176	1120	66.7
C	1.26	13.3	173	0.186	928	69.8

The percentages in parentheses are error estimates.

Table 3. Calculated noise voltages of the tuned coils

Coil	R_s in Ω at 6.245 MHz	Noise voltages (in nV) Coil†	Electric‡	Magnetic§	Total noise voltage from coil circuit*
A	0.129	0.96	0.06	0.10	0.97
B	0.651	0.96	0.13	0.10	0.97
C	6.31	0.94	0.22	0.07	0.97
E	0.020	0.71	0.10	0.65	0.97

*$N_v = \{4\kappa T\Delta f[F_1^2(R_s + \mathrm{Re}(Z_{mag})) + F_2^2 R_e]\}^{1/2}$.
†$F_1(4\kappa T\Delta f R_s)^{1/2}$, where $\Delta f = 1$ Hz, $T = 295$ K.
‡$F_2(4\kappa T\Delta f R_e)^{1/2}$.
§$F_1[4\kappa T\Delta f\,\mathrm{Re}(Z_{mag})]^{1/2}$.

the noise voltage due to R_s for the solenoids dominates over the other noise voltages. At higher frequencies, magnetic noise voltage would be more important because Z_{mag} is proportional to ω^2.[15]

The electric noise voltages increase from coil A to coil C, but the coil noise voltages vary only slightly despite a fiftyfold increase in R_s from Coils A–C. This phenomenon demonstrates the overall importance of transfer factors in determining noise voltages. F_1 decreases drastically from Coil A to C and coil noise scales as F_1^2. The slight drop in coil noise voltage for Coil C is due to the increasing contribution of electric noise voltage. The coil noise voltage for Coil C drops slightly to accommodate the increase in electric noise voltage as C_s and C_p are adjusted to tune the coil circuit to 57 Ω.

DISCUSSION

The use of transfer functions derived from an equivalent circuit is an unusual but useful approach for understanding and optimizing coil performance. We believe that these experiments validate the method of analysis we have developed. The calculated value of the transfer function F_1 was shown to agree with measurements for a series of three small solenoid coils. The calculated total noise voltage was used in the determination of relative SNR which was verified by an MR imaging experiment using the same three solenoids.

The use of transfer functions in understanding SNR is illustrated by the data of Table 2. At first glance, it is surprising that the calculated and measured SNR's are essentially independent of B_1 [see Eq. (10)] which is proportional to the number of turns, N, in the solenoids (A-7, B-15, and C-36). B_1, however, is only one of three factors in Eq. (11). Another factor, N_v, is constant because all three coils are tuned to the same impedance. These coils were designed, however, with wire diameter, d_w, inversely proportional to the number of turns. Since $R_s \propto 1/d_w$ and $R_s \propto$ wire length, then $R_s \propto N^2$ and $F_1 \propto 1/R_s^{1/2} \propto N$. Thus for these three solenoids, $F_1 B_1$ is constant and we expect SNR to be independent of N. When R_s is the dominant loss mechanism, the relative SNR of a series of coils with equal geometry would depend only on their empty coil Q values. Thus for this special case, SNR $\propto Q$, and the SNR independence of N is equivalent to Q independence of N, which was noted by Medhurst.[16]

This independence of SNR and N has also been reported to occur for simple surface coils at high frequencies (~60 MHz).[17] Under conditions where magnetic noise voltage dominates, both the signal and noise are propagated by the same transfer factor, F_1. Signal remains proportional to N, but $\mathrm{Re}(Z_{mag})$ is proportional to N^2, similar to R_s in the preceding solenoid example. Thus SNR performance of multiple-turn surface coils at high frequencies also remains relatively independent of the number of turns.

Overall, this type of analysis reveals which aspects of coil design are limiting to overall performance. For example, reducing Coil C's electric noise voltage (by inserting a Faraday shield) would improve its performance more than Coil A's. The improvement would not be very significant, however, because Table 3 shows that coil noise voltage predominates for all three coils. A more instructive example is Coil E for which this analysis shows that magnetic and coil noise voltages are almost equal. Doubling the conductor diameter from 12.5 to 25 mm could reduce R_s by as much as one half (provided tuning capacitor losses are insignificant), but the SNR would improve at most by only 20%. Further increases in conductor diameter would provide even less improvement in SNR (as well as being impractical) because the magnetic noise voltage would dominate.

As shown in the Appendix, the transfer function method of calculating relative SNR is, under specific conditions which neglect R_e, equivalent to other expressions in the literature.[2,4] The quantitative treatment of the noise voltages from all energy dissipative elements is a major advantage for our technique which makes it suitable for coil optimization throughout the MR imaging frequency range. Of course, the specific geometry of the coil's magnetic and electric fields is still important in determining coil performance. They determine not only the magnitude of the components of the equivalent circuit, but also signal uniformity. For example, Hayes and Axel[9] have investigated the depth at which SNR from various diameter surface coils exceeds that of a standard head coil.

Our method provides a complementary tool. Provided the equivalent circuit component values are known, it is possible to calculate how closely a coil's performance at a particular frequency approaches the ideal SNR *of that geometry*. For optimum performance, the noise voltage from $\mathrm{Re}(Z_{mag})$ should predominant over that from R_s and R_e. Thus a coil-specific figure of merit can be derived as

$$\mathrm{FOM} = \frac{N_v(\mathrm{mag})}{N_v(\mathrm{circuit})} = \sqrt{\frac{F_1^2 \mathrm{Re}(Z_{mag})}{F_1^2(R_s + \mathrm{Re}(Z_{mag})) + F_2^2 R_e}}$$

An optimum coil would have $R_s = R_e = 0$, and FOM = 1.0. Because of their large R_s, the three solenoids have an FOM of only 0.07–0.10, falling far short of an ideal, lossless conductor. The half-saddle head coil (Coil E) scores somewhat better with a FOM of 0.68. This comparison also illustrates the fact that since $\mathrm{Re}(Z_{\mathrm{mag}})$ depends on sample radius to the fifth power,[5] at a given frequency, small coils are harder to optimize than large coils.

This figure of merit is, however, coil specific. For SNR in MR imaging, the other factors of Eq. (10) are important, including the three dimensional distribution of B_1, the operating frequency, ω_0, and other geometric factors. In the long term, it would be advantageous to calculate coil performance completely without resorting to construction and measurement. In terms of the equivalent circuit model, this would require detailed calculation of the electric and magnetic field distributions of a coil and the specific evaluation of many parameters including R_e, R_s, C_1, C_2 and $\mathrm{Re}(Z_{\mathrm{mag}})$. When, or if, such calculations are possible, the transfer function technique described in this paper could be used to assess and optimize coil SNR performance completely by calculation.

APPENDIX

The expression for SNR developed as Eq. (9) can be shown to be identical to familiar expressions already in the literature. Hoult[4] has shown that his expression is similar to that of Abragam[2]:

$$\mathrm{SNR} = K\eta M_0\left(\frac{Q\omega_0 V_c}{4\kappa T\Delta f F}\right)^{1/2} , \qquad (15)$$

where V_c is the coil volume, K is a proportionality constant, F is the preamplifier noise power factor and η is the fraction of the total magnetic field within the sample, the "filling factor." Removing constants of proportionality, but retaining all coil and sample specific terms simplifies this equation to

$$\mathrm{SNR} \propto \eta M_0 (Q\omega_0 V_c)^{1/2} . \qquad (16)$$

Equation (9) can be shown rigorously to be identical to this expression with the following algebraic manipulation. First, an expression for $\mathrm{Re}(Z_{\mathrm{gh}})$ is derived from Eqs. (7) and (8):

$$\mathrm{Re}(Z_{\mathrm{gh}}) = F_1^2(R_s + \mathrm{Re}(Z_{\mathrm{mag}})) + F_2^2 R_e , \qquad (17)$$

where all quantities which are functions of frequency have been evaluated at ω_0. To make this comparison, the term involving R_e must be set to zero because Eq. (15) does not include coil–sample electric field interactions. Equation (17) can be rearranged to

$$F_1^2 = \frac{\mathrm{Re}(Z_{\mathrm{gh}})}{R_s + \mathrm{Re}(Z_{\mathrm{mag}})} . \qquad (18)$$

The quality factor, Q, is introduced as $\omega_0 L/(R_s + \mathrm{Re}(Z_{\mathrm{mag}}))$ whence

$$F_1 = \left(\frac{\mathrm{Re}(Z_{\mathrm{gh}})Q}{\omega_0 L}\right)^{1/2} . \qquad (19)$$

Substituting F_1 from Eq. (19) and ϵ from Eq. (10) into Eq. (9), yields the required expression for SNR:

$$\mathrm{SNR} = \left(\frac{\mathrm{Re}(Z_{\mathrm{gh}})Q}{\omega_0 L}\right)^{1/2} \frac{\omega_0 B_1 M_0 V_s \cos\omega_0 t}{N_v} . \qquad (20)$$

For coils tuned to 50 Ω, $\mathrm{Re}(Z_{\mathrm{gh}})$ is constant and, from Eq. (8), $N_v \propto \sqrt{\mathrm{Re}(Z_{\mathrm{gh}})}$. Removing constants of proportionality and using two additional relationships,[4] $B_1 \propto (\eta L/V_s)^{1/2}$ and $V_s \propto \eta V_c$ permits simplification of Eq. (19) to

$$\mathrm{SNR} \propto \eta M_0 (Q\omega_0 V_c)^{1/2} , \qquad (21)$$

which is identical to Eq. (16).

REFERENCES

1. van Heteren, J.G.; Henkelman, R.M.; Bronskill, M.J. Equivalent Circuit for Coil-Patient Interactions in Magnetic Resonance Imaging. *Magn. Reson. Imaging.* 5:93–99; 1987.
2. Abragam, A. *The Principles of Nuclear Magnetism.* Oxford: Clarendon; 1961.
3. Clark, W.G.; McNeil, J.A. Single Coil Series Resonant Circuit for Pulsed Nuclear Resonance. *Rev. Sci. Instrum.* 44(7):844–851; 1973.
4. Hoult, D.I.; Richards, R.E. The Signal-to-Noise Ratio of the Nuclear Magnetic Resonance Experiment. *J. Magn. Reson.* 24:71–85; 1976.
5. Hoult, D.I.; Lauterbur, P.C. The Sensitivity of the Zeugmatographic Experiment Involving Human Samples. *J. Magn. Reson.* 34:425–433; 1979.
6. Libove, J.M.; Singer, J.R. Resolution and Signal-to-Noise Relationships in NMR Imaging in the Human Body. *J. Phys. (E)* 13(1):38–44; 1980.
7. Grist, T.M.; Hyde, J.S. Resonators for *in-vivo* ^{31}P NMR at 1.5 T. *J. Magn. Reson.* 61:571–578; 1985.
8. Hayes, C.E.; Edelstein, W.A.; Schenck, J.F.; Mueller, O.M.; Eash, M.E. An Efficient, Highly Homogeneous Radiofrequency Coil for Whole-Body NMR Imaging at 1.5T. *J. Magn. Reson.* 63:622–628; 1985.
9. Hayes, C.E.; Axel, L. Noise Performance of Surface Coils for Magnetic Resonance Imaging at 1.5T. *Med. Phys.* 12(5):604–607; 1985.
10. Sergiadis, G. Performance Evaluation of Whole-Body NMR Scanner Antenna Systems. *Magn. Reson. Med.* 2:328–335; 1985.
11. Motchenbacher, C.D.; Fitchen, F.C. *Low-Noise Electronic Design.* New York: John Wiley and Sons; 1973.

12. Fitzsimmons, J.R.; Thomas, R.G.; Mancuso, A.A. Proton imaging with Surface Coils on a 0.15T Resistive System. *Magn. Reson. Med.* 2:180–185; 1985.
13. Edelstein, W.A.; Bottomley, P.A.; Pfeifer, L.M. A Signal-to-Noise Calibration Procedure for NMR Imaging Systems. *Med. Phys.* 11(2):180–185; 1984.
14. Henkelman, R.M. Measurement of Signal Intensitites in the Presence of Noise in MR Images. *Med. Phys.* 12(2):232–233; 1985.
15. Edelstein, W.A.; Glover, G.H.; Hardy, C.J.; Redington, R.W. The Intrinsic Signal-to-Noise Ratio in NMR Imaging. *Magn. Reson. Med.* 3:604–618.
16. Medhurst, R.G. H.F. Resistance and Self-Capacitance of Single Layer Solenoids. *Wireless Engineer* 24:35–43, 80–92; 1947.
17. Edelstein, W.A.; Foster, T.H.; Schenck, J.F. The Relative Sensitivity of Surface Coils to Deep Lying Tissues, Proceedings, 4th Annual Meeting, Society of Magnetic Resonance in Medicine, Aug. 19–23, 1985, London, p. 964, Soc. of Magn Reson in Med., Berkeley Calif.